Supplementary Material

Table 1: Different datasets and resolution used in this study

Dataset	Types	Variables	Spatial Resolution	Characteristics	Cover period
ORAS5	Ocean reanalysis	SST, sea surface salinity, zonal and meridional wind stress, zonal and meridional velocity	0.25ºx0.25º	NEMO version 3.4 ocean model, 75 vertical levels, forced with ERA-40 (before 1979), ERA-Interim (1979-2015) and real-time Numerical Weather Prediction (NWP, 2015-preset), with bulk formula + wave forcing, HadISST and OSTIA observations	1980 - 2023
ERA5	Atmospheric reanalysis	SST, zonal and meridional wind components	0.25ºx0.25º 137 levels to 1Pa	Copernicus Climate Change Service (C3S) 137 levels to 1 Pa, HadISST, OSTIA with bulk formula, including global atmosphere, land surface and ocean waves	1980 - 2023
HadISST	Station observations	SST	1º x 1º		1980 - 2023
OSTIA	Satellite	SST	0.05ºx0.05º	Advance Very High-Resolution Radiometers (AVHRRs), Along Track Scanning Radiometers (ATSRs), Sea and Land Surface Radiometer (SLSRs), 2, 3, 4 levels	1982 - 2022
Global Ocean reanalysis (GLORYS)	Ocean reanalysis	SST, zonal and meridional wind stress, zonal and meridional velocity, sea surface salinity, sea level anomaly	0.083ºx0.083º	GLORYS12 version 1 ocean physics model, (1993-present), 50 vertical levels, forced with ERA-Interim and a real-time global	1993-2020

				forecasting CMEMS system	
Global Ocean Biogeochemistry Analysis and Forecast	Ocean Analysis and Forecast	Oxygen (O2), nitrate (NO3)	0.25ºx0.25º	NEMO version 3.6, forced with GLOBAL_ANALYSIS_FORECAST_PHYS_001_024 at daily frequency	2020-2021
NOAA	Satellite	Chlorophyll-a concentration	0.042ºx0.042º	Regular longitude-latitude grid, Single level and daily frequency	1997-2023
NOAA-CPC	Climate indices	Niño 3.4 and NAO	Time-series		1982-2023

Table S2: Upwelling indices used in this study

Acronyms	Full Name	Definition	Formula	Unit
$M_{(x)}$, $M_{(y)}$	Zonal Ekman and Meridional Transport	Upwelling index related to offshore wind stress	$M_{(x)} = \frac{\tau^y}{\rho_w f}$ $M_{(y)} = -\frac{\tau^x}{\rho_w f}$	$m^2.s^{-1}$
W_{scd}	Wind-stress curl driven upwelling (Ekman pumping velocity)	Upwelling related to coastal divergence	$W_{scd} = \frac{1}{\rho_w f}\left(\frac{\partial \tau^y}{\partial x} - \frac{\partial \tau^x}{\partial y}\right)$	$m.day^{-1}$
W_t	Total wind-driven upwelling index	Sum of offshore Ekman transport velocity and inshore Ekman (offshore divergence) pumping velocity (coastal divergence)	$W_t = M_{(x,y)} + W_{scd}$	$m.day^{-1}$
CUI	Cumulative upwelling index	Integrated daily upwelling index over the upwelling cycle	$CUI(t) = \sum_{i=0}^{t} UI(i).\Delta t$	$m^2.s^{-1}$ and ºC
TUM	Total upwelling magnitude	Cumulative upwelling index from the start to the end datesof upwelling season	$TUM = \sum_{END}^{STI} CUI(t)$	$m^2.s^{-1}$ and ºC
SST_{index}	SST gradient	SST difference between offshore and coastal areas	$SST_{ui} = SST_{open-ocean} - SST_{coast}$	ºC

T_g, $UI_{(SLA,SSH)}$	Onshore geostrophic Transport and coastal upwelling index based on the geostrophic flow	Component of geostrophic current that flows from open-ocean to the coast, Coastal divergence based on SLA and SSH	$T_g = \frac{g}{f}\frac{\partial \eta_{al} - \partial \eta_{on}}{d} MLD$ $UI_{(SLA,SSH)} = \left(\frac{\partial vg}{\partial x} + \frac{\partial ug}{\partial y}\right)$ Where $ug = -\frac{g}{f}\frac{\partial \eta}{\partial y}$, $vg = \frac{g}{f}\frac{\partial \eta}{\partial x}$, η is SSLA or SSH	$m^2.s^{-1}$

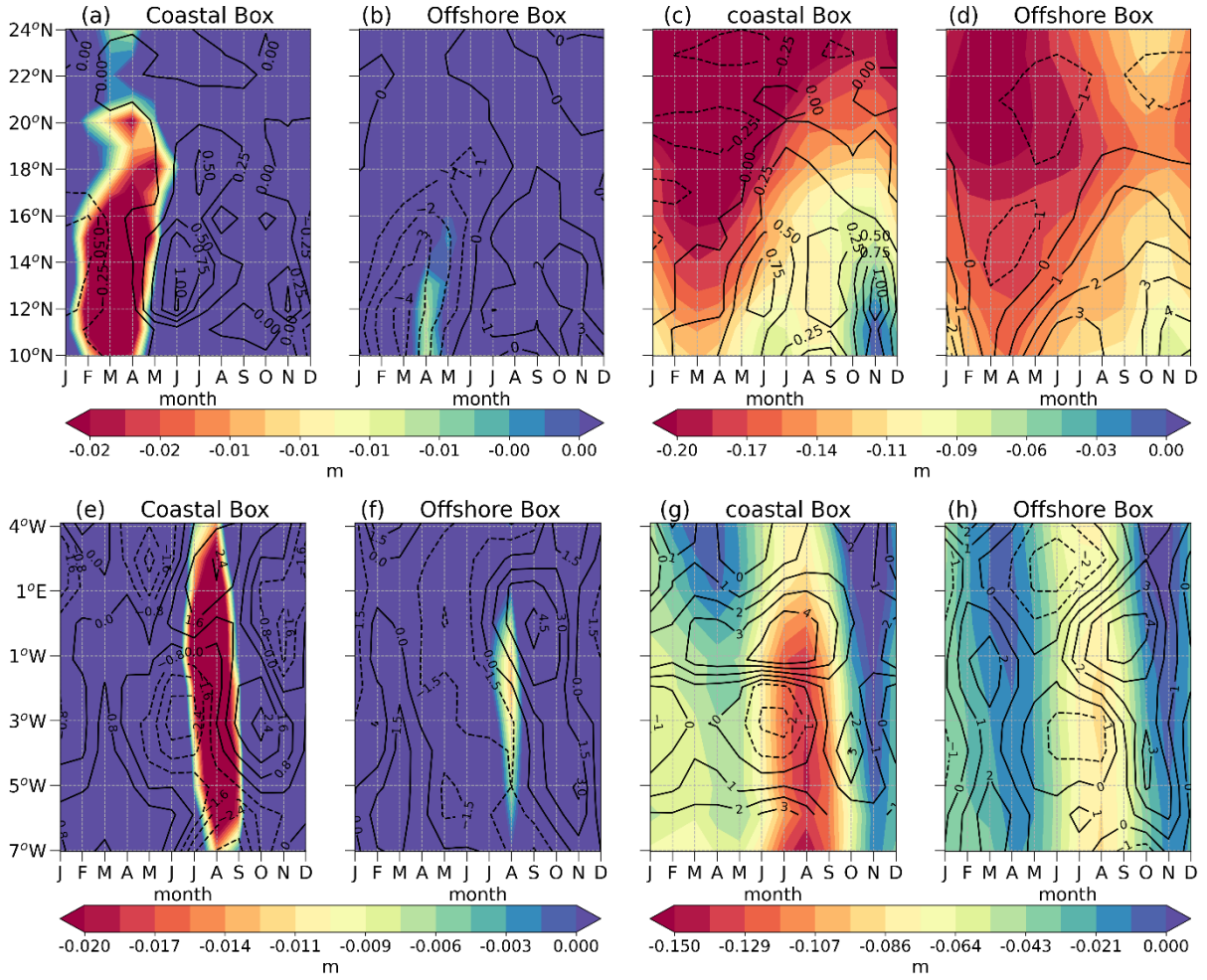

Figure S1: a-b Seasonal sea level anomaly (shading, m) and the divergence computed with sea Level Anomaly (SLA) (contour, m^2 s^{-1}) in the Senegal-Mauritania coastal Upwelling System (SMUS). c-d Sea surface height (shading, m) and divergence in computed with Sea Surface Height (m^2 s^{-1}) in the Senegal-Mauritania coastal Upwelling System (SMUS). a-b Seasonal sea level anomaly (shading, m) and the divergence computed with sea Level Anomaly (SLA) (contour, m^2 s^{-1}) in the Gulf of Guinea coastal Upwelling System (GGUS). c-d Sea surface height (shading, m) and divergence in computed with Sea Surface Height (m^2 s^{-1}) in the Gulf of Guinea coastal Upwelling System (GGUS). Warm colour denotes negative SLA or SSH resulting the favourable upwelling conditions including coastal trapped waves (CTWs) propagating poleward. Cool colour denotes the positive SLA or SSH resulting favourable downwelling events including Kelvin waves arriving from the equatorward and generating poleward CTWs.

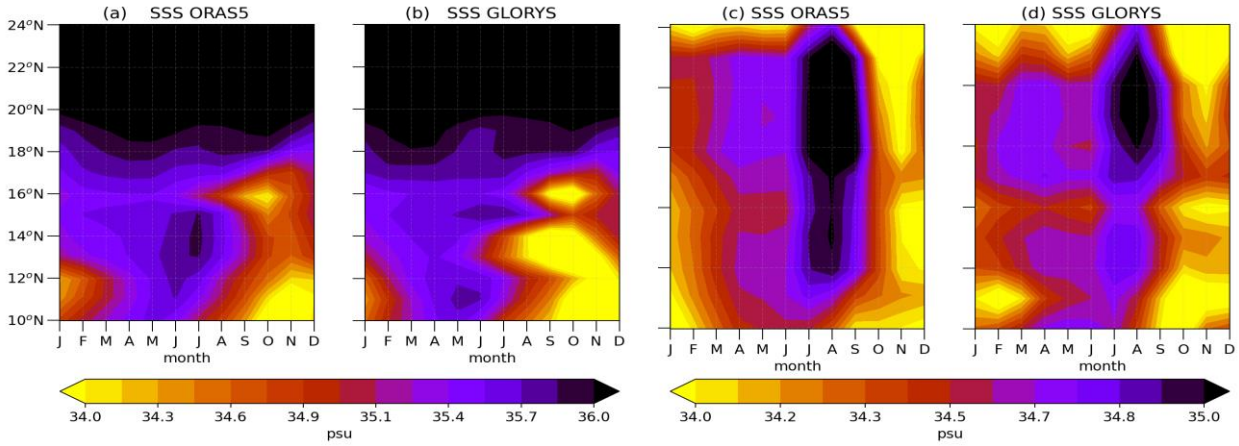

Figure S2: Seasonal variability of Surface salinity in the Senegal-Mauritania (a, b) and Gulf of Guinea (c,d) coastal upwelling systems. Warm black colour denotes the concentration of sea surface salinity. a, c Five generation of ocean reanalysis system (ORAS5) products. b, d Global physics ocean reanalysis (GLORYS) products.

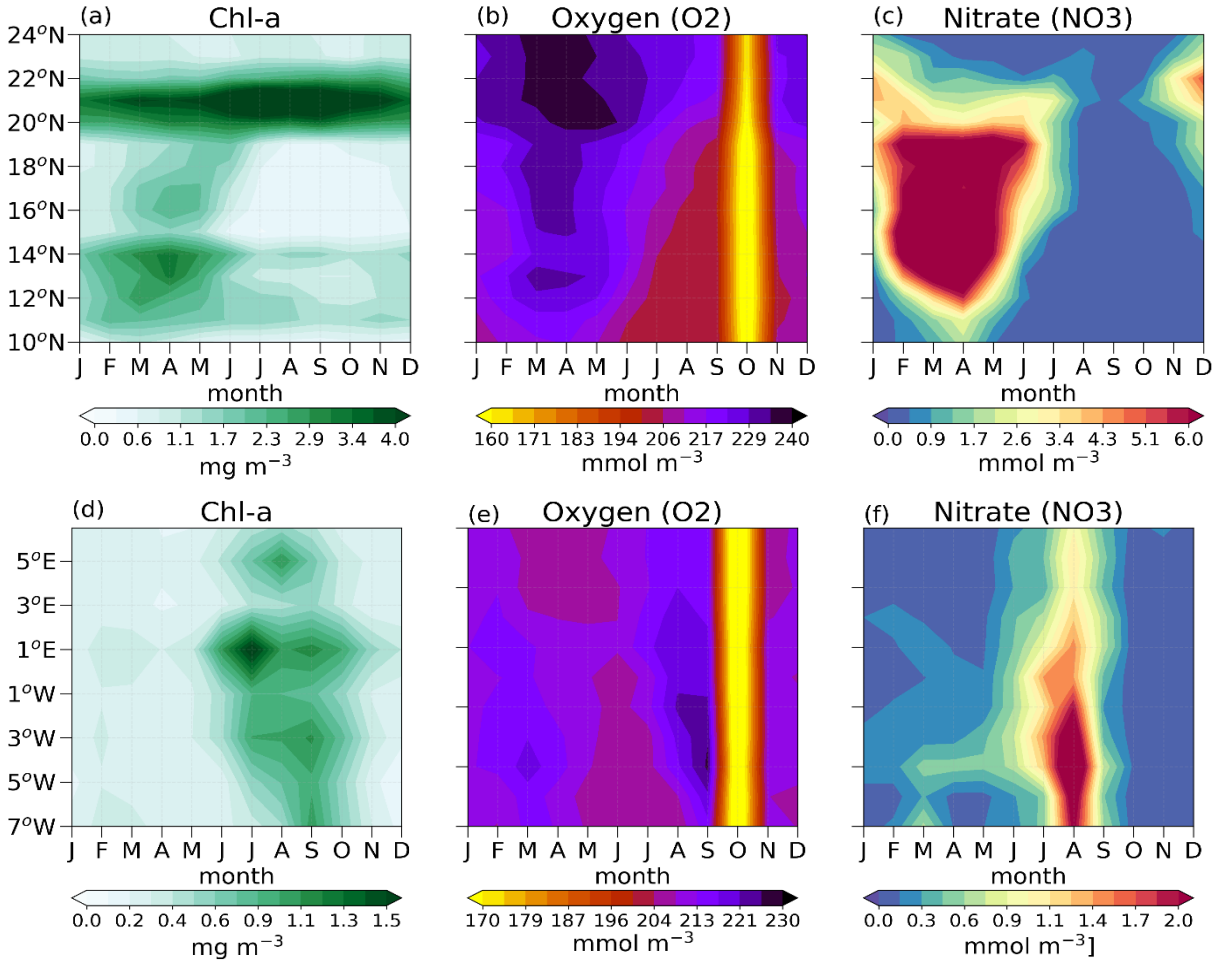

Figure S3: a, b, c Seasonal variability of chlorophyll-a concentration, dissolved oxygen and Nitrate in the Senegal-Mauritania Upwelling System (SMUS). d, e, f Seasonal variability of chlorophyll-a concentration, dissolved oxygen and Nitrate in the Gulf upwelling system (GGUS). Warm green colour (a, d) shows the strong chlorophyll-a concentration. Yellow colour (b, e) shows minimum peak of dissolved oxygen which coincides with upwelling transition month (October) in both upwelling systems. Warm colour (c, f) denotes strong concentration of nitrate with coincides with the maximum peak of upwelling in each upwelling system.

The seasonal variability of sea surface salinity (Fig. S2), dissolved oxygen, nitrate and chlorophyll-a concentration (Fig. S3) was analysis as additional upwelling indicators of upwelling in the two systems. In the SMUS, the maximum surface salinity is observed in the permanent upwelling region over 18ºN and reaches in the southern area during the peaks of local upwelling. The spatial variability of salinity seems to be related to the large circulation of Atlantic Ocean surface water masses than upwelling winds driving by the North Atlantic Subtropical and Tropical gyres (Benazzouz et al., 2014). The northern maximum Salinity (>35 psu) can be linked to the North Atlantic Central dense Waters (SACWs). Whereas, the relative weak surface salinity (>35 psu) seems to be related to the Southern Atlantic Central warm Water masses (SACWs) salinity. The maximum peaks of dissolved oxygen (O2), nitrate (NO3) and chlorophyll-a concentration (Chl) are well correlated to the seasonality of upwelling (December-June). The main concentration of O2 is observed in the permanent upwelling region when NO3 supply peaks in the seasonal upwelling with intense upwelling events (March-April-May). However, the minimum peaks of these variables coincide with the highest SST (September-October). In the GGUS the Figs. S7 c, d and S8 d, f show that the temporal and spatial distribution of the surface salinity, O2 and NO3 are directly connected to upwelling season (JAS). This connection between upwelling events and peaks of sea surface salinity (>34 psu) can be explained by considering the physical and oceanographic processes associated with upwelling. The deep ocean waters that rise to the surface are typical stable and more saline than the surface layer often diluted by precipitation and river runoff. When the upwelling occurs, it replaces this surface waters with saltier waters leading to an increase in surface salinity and nutrients. Compared to the SMUS, the concentration of the three variables is more important in SMUS than in the GGUS because of the intensity and duration of upwelling.

Differential Drivers of SMUS and GGUS Variability

The correlation tables also highlight the differing roles of other climate modes. For example, the North Atlantic Oscillations (NAO) shows a moderate influence on SMUS upwelling, particularly during JJA (r = -0.33 for SST-UI), consistent with previous studies that link positive NAO phases to intensified trade winds along the Northwest African coast. The Atlantic Meridional Mode (AMM) and North Tropical Atlantic (NTA) have significant impacts on GGUS, with correlations reaching r = -0.58 (AMM and SST-UI, JJA), confirming that Atlantic meridional modes modulate interhemispheric SST gradients that influence equatorial and coastal winds. The Southern Oscillations Index SOI is positively correlated with upwelling in both regions during DJF, reflecting its inverse relationship with El Niño events.

These results demonstrate the complexity of climate–upwelling interactions in this region and highlight the importance of considering both seasonality and regional specificity in assessing climate impacts on coastal ocean dynamics.

Table S3: Lag/lead correlation coefficients between climate indices and UIs during winter period

DJF	Ekman Transport Index in SMUS					SST Upwelling Index in GGUS				
	Lag 2	Lag 1	Lag 0	Lead 1	Lead 2	Lag 2	Lag 1	Lag 0	Lead 1	Lead 2
ENSO+	-0.51	0.91	0.90	0.84	0.81	0.14	0.97	0.43	0.31	0.26
ENSO-	0.99*	0.98	-0.35	-0.99*	-0.98	-0.68	-0.51	-0.46	0.60	0.80
NAO+	-0.99*	-0.49	-0.99*	0.57	0.97	0.92	-0.49	0.94	-0.20	-0.80

NAO-	0.52	0.96	-0.48	-0.99*	-0.44	0.30	-0.84	-0.35	0.75	0.97
SOI+	-0.96	-0.32	-011	0.50	0.93	0.34	0.96	-0.74	0.42	-0.84
SOI-	0.34	0.85	-0.19	0.88	0.58	-083	0.52	0.91	-0.24	0.93
ATL3+	0.10	-0.91	-0.96	-0.98	-0.84	-0.60	0.55	0.67	0.72	0.43
ATL3-	0.20	0.23	-0.91	-0.82	-0.45	0.32	0.29	0.99*	0.43	0.83
AMM+	-0.89	-0.81	0.72	0.99*	0.99*	0.99*	0.52	-0.40	-0.87	-0.96
AMM-	-0.41	-0.09	0.99*	0.38	-0.15	0.79	0.56	-0.86	-0.78	-0.34
AMO+	0.06	0.66	-0.55	0.77	-0.64	-0.59	0.99*	0.12	-0.18	0.009
AMO-	0.88	-0.99*	-0.97	-0.91	0.59	-0.82	0.36	0.23	0.79	-0.99*
PDO+	-0.85	-0.99*	-0.95	-0.82	0.0006	0.59	0.94	0.99*	0.55	0.37
PDO-	0.96	0.60	-0.88	0.48	-0.72	-0.99*	-0.46	0.94	-0.62	0.60
ONI+	-0.82	-0.40	0.99*	0.95	0.90	0.32	-0.22	-0.80	-0.59	-047
0NI-	0.78	-0.94	-0.89	-0.98	-0.98	-0.81	-0.06	0.68	0.45	0.45
NOI+	-0.33	-0.98	-0.61	0.98	0.52	-0.74	0.23	0.97	-0.22	-0.99*
NOI-	-0.13	0.92	0.80	-0.73	-0.99*	0.85	-0.27	-0.97	-0.07	0.72
PNA+	-0.67	-0.92	0.99*	0.92	0.95	0.26	0.99*	-0.82	-0.64	-0.99
PNA-	0.88	0.63	0.95	0.96	-0.32	-0.99*	-0.89	-0.99*	-0.99*	-0.09
NTA+	-0.94	-0.99*	0.34	-0.89	0.49	0.70	0.88	-0.72	0.99*	-0.05
NTA-	0.75	0.64	-0.30	0.69	0.72	0.33	0.47	-0.77	0.41	0.37

Table S4: Lag/lead correlation coefficients between climate indices and Us during spring period

MAM	Ekman transport Index					SST upwelling Index				
	Lag 2	Lag 1	Lag 0	Lead 1	Lead 2	Lag 2	Lag 1	Lag 0	Lead 1	Lead 2
ENSO+	0.48	0.53	0.58	0.55	0.47	0.48	0.43	0.38	0.50	0.41
ENSO-	0.82	0.63	0.73	0.81	0.63	-0.79	-0.59	-0.69	-0.77	-0.59
NAO+	-0.99*	-0.83	-0.99*	0.13	-0.84	0.99*	0.72	0.99*	-0.29	0.92
NAO-	0.99*	0.46	-0.99*	-0.75	0.91	-0.99*	-0.64	0.93	0.87	-0.80
SOI+	-0.89	-0.93	-0.98	-0.80	0.79	0.85	0.64	0.95	0.41	-0.99
SOI-	-0.47	-0.93	-0.98	-0.80	0.79	0.85	0.64	0.95	0.41	0.98
ATL3+	-0.14	0.22	0.02	-0.11	-0.62	-0.77	-0.95	-0.87	-0.80	-0.35
ATL3-	-0.43	-0.82	-0.69	-0.34	0.96	0.13	0.96	0.88	0.62	0.82
AMM+	-0.75	-0.89	-092	-0.58	-0.99*	0.99*	0.93	0.90	0.99*	0.64
AMM-	0.88	0.99	0.68	0.40	0.91	-0.68	-0.21	0.53	-0.98	-0.63
AMO+	-0.21	-0.39	0.06	-0.09	-0.06	-0.16	0.03	-0.41	-0.27	-0.31
AMO-	0.59	-0.13	0-93	0.99	0.32	-0.34	-0.15	-0.99*	-0.98	0.04
PDO+	0.99*	-0.63	-0.89	-0.87	0.50	-0.99*	0.44	0.97	0.96	-0.28
PDO-	0.01	0.97	0.99*	-0.30	-0.89	-0.52	-0.95	-0.84	0.75	0.53
ONI+	-0.41	-0.27	-0.23	-0.26	-0.20	0.90	0.83	0.81	0.82	0.79
ONI-	0.44	0.44	0.26	0.06	-0.87	-0.15	-0.15	0.04	0.25	0.69
NOI+	-0.99*	-0.23	-0.31	-0.75	-0.66	0.70	-0.41	0.83	0.19	0.06
NOI-	0.99*	0.52	-0.22	0.99*	-0.05	-0.96	-0.82	-0.18	-0.94	-0.35
PNA+	-0.99*	-0.79	-0.97	-0.15	0.97	0.99*	0.80	0.96	0.17	-0.97
PNA-	0.60	-0.82	0.64	-0.68	0.97	-0.82	0.61	-0.84	0.43	-0.85
NTA+	0.78	-0.66	-0.98	-0.99*	-0.97	-0.85	0.57	0.95	0.99*	0.99*
NTA-	-0.99*	-0.99*	0.19	0.96	0.99*	0.97	0.96	-0.44	-0.99*	-0.98

Table S5: Lag/lead correlation coefficients between climate indices and UIs during summer period

JAS	Ekman Transport					SST Upwelling Index				
	Lag 2	Lag 1	Lag 0	Lead 1	Lead 2	Lag 2	Lag 1	Lag 0	Lead 1	Lead 2
ENSO+	0,57	0.92	0.93	0.15	-0.51	0.55	0.008	-0.006	0.97	0.61
ENSO-	-0.99*	-0.38	0.99*	0.99*	0.94	0.75	0.95	-0.75	-0.60	-0.87
NAO+	0.15	0.78	-0.99*	0.97	-0.25	0.81	-0.91	0.57	-0.22	-0.74
NAO-	-0.67	-0.45	0.97	0.68	-0.81	-0.13	0.97	-0.44	-0.99*	0.97
SOI+	-0.51	-0.31	-0.41	-0.99*	-0.45	-0.27	0.90	-0.37	0.63	0.95
SOI-	-0.97	0.87	0.82	-0.92	-0.57	0.83	-0.98	-0.58	0.99*	0.27
ATL3+	0.92	-0.76	-0.98	-0.99*	-0.99*	0.89	0.007	-0.48	-0.69	-0.71
ATL3-	-0.95	-0.80	-0.64	-0.62	-0.53	-0.93	-0.27	-0.03	-0.005	0.10
AMM+	0.97	-0.62	-0.78	-0.88	-0.91	-0.72	-0.33	-0.12	0.07	0.12
AMM-	0.11	-0.93	0.99*	-0.30	-0.95	0.06	-0.98	-0.97	0.46	0.88
AMO+	-0.86	-0.90	-0.09	0.85	0.88	-0.47	-0.39	0.99*	0.49	0.42
AMO-	-0.89	0.62	0.35	-0.99*	0.43	0.83	0.37	-0.99*	0.44	0.57
PDO+	0.61	0.66	0.86	0.99*	-0.47	-0.71	0.66	-.60	0.08	-0.92
PDO-	0.99*	-0.51	-0.98	0.64	0.94	-0.83	-0.09	0.90	-0.07	-0.57
ONI+	0.76	0.75	0.62	0.69	0.77	0.59	0.61	0.74	0.67	0.57
0NI-	0.71	0.98	0.96	0.99	0.98	0.19	-0.41	-0.32	-0.47	-0.38
NOI+	-0.52	0.78	0.86	0.93	0.95	0.99*	0.06	-0.09	-0.24	-0.31
NOI-	-0.42	-0.31	-0.27	-0.26	-0.27	0.18	0-07	0.03	0.01	0.03
PNA+	-0.41	-0.58	0.96	-0.34	-0.79	-0.76	0.94	-0.51	-0.81	-0.80
PNA-	0.78	-0.57	-0.93	0.78	0.78	-0.91	0.35	0.99*	-0.61	-0.61
NTA+	0.88	0.93	0.86	0.94	0.68	0.19	0.07	0.23	0.04	-0.90
NTA-	-0.91	-0.98	-0.99*	-	0.58	0.15	0.41	0.63	-	0.35

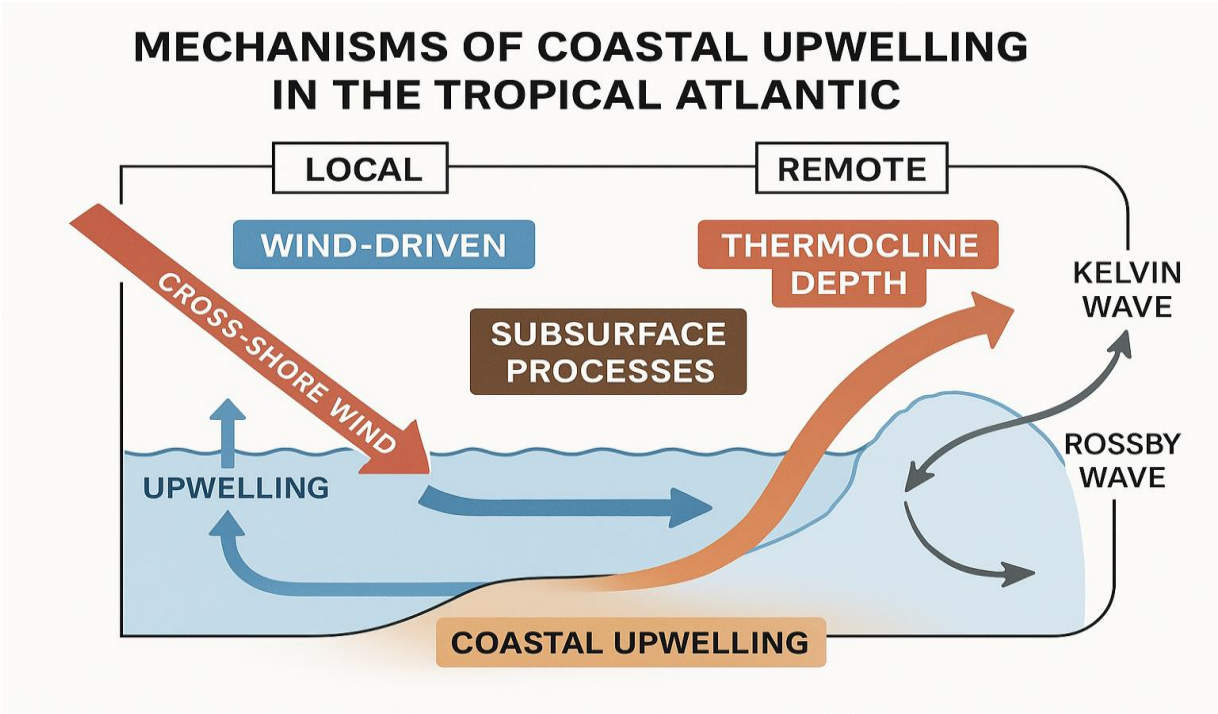

Figure S5: Summary of Coastal Upwelling Mechanisms in the Tropical Atlantic.

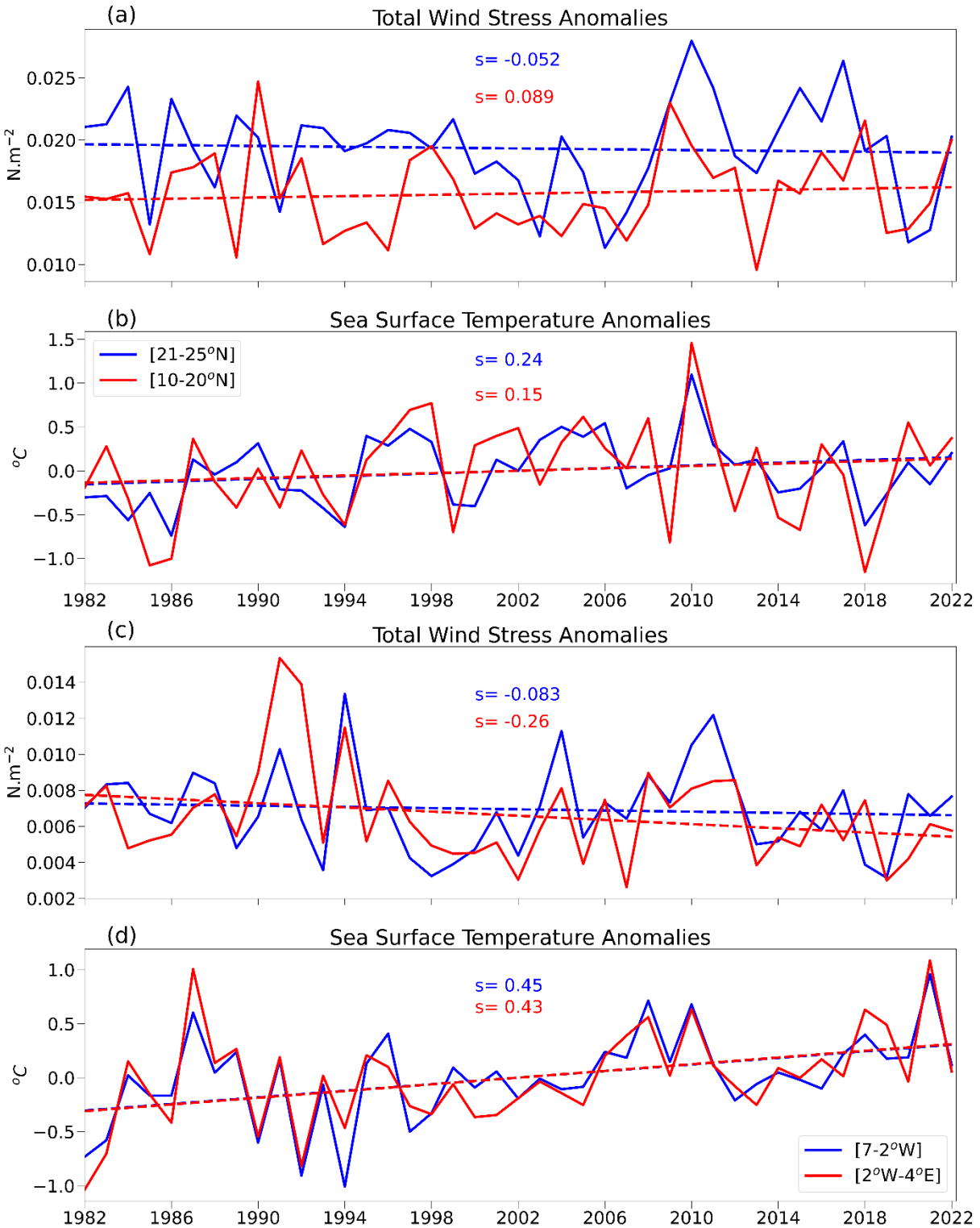

Figure S4: a, b Historical trends of meridional wind stress and sea surface temperature anomalies in the Senegal-Mauritania upwelling system (SMUS). Blue line denotes the time series of the permanent upwelling region, while red line indicates the time series of the seasonal upwelling region. Historical trends of meridional wind stress and sea surface temperature anomalies in the Gulf of Guinea upwelling system (GGUS). Blue line denotes the time series of the eastern of Cape Palmas, while red line indicates the time series of the eastern of Cape Three Points.